Quantum chemical study of the atmospheric C2H5C(O)OONO2 (PPN) molecule and of the C2H5C(O)OO and C2H5C(O)O radicals

ARTICLE *in* JOURNAL OF MOLECULAR STRUCTURE THEOCHEM · MAY 2008

Impact Factor: 1.37 · DOI: 10.1016/j.theochem.2008.01.015

2 AUTHORS:

María Badenes
National University of La Plata
20 PUBLICATIONS **122** CITATIONS
SEE PROFILE

Carlos J. Cobos
National Scientific and Technical Research …
126 PUBLICATIONS **3,054** CITATIONS
SEE PROFILE

ELSEVIER

Journal of Molecular Structure: THEOCHEM 856 (2008) 59–70

THEO CHEM

www.elsevier.com/locate/theochem

Quantum chemical study of the atmospheric $C_2H_5C(O)OONO_2$ (PPN) molecule and of the $C_2H_5C(O)OO$ and $C_2H_5C(O)O$ radicals

María P. Badenes *, Carlos J. Cobos

Instituto de Investigaciones Fisicoquímicas Teóricas y Aplicadas (INIFTA), Departamento de Química, Facultad de Ciencias Exactas, Universidad Nacional de La Plata, CONICET, CICPBA, Casilla de Correo 16, Sucursal 4, 1900 La Plata, Argentina

Received 20 December 2007; received in revised form 15 January 2008; accepted 16 January 2008
Available online 26 January 2008

Abstract

Ab initio and density functional calculations have been performed on atmospheric peroxypropionyl nitrate, $C_2H_5C(O)OONO_2$ (PPN) molecule and its radical decomposition products $C_2H_5C(O)OO$ and $C_2H_5C(O)O$. Potential barriers for the internal rotations have been computed at the B3LYP/6-311++G(d,p) level of theory. Geometries, harmonic vibrational frequencies and thermochemical properties of stable rotational conformers and transition states have been calculated at the B3LYP/6-311++G(3df,3pd) and G3MP2B3 levels. For PPN, the results shown a structure in which the atoms nearest to the O—O bond are in approximately perpendicular planes, $\tau(COON) = 85.9°$. The standard enthalpies of formation at 298 K have been calculated using isodesmic reactions at the G3MP2//B3LYP/6-311++G(3df,3pd) level of theory. The resulting values for PPN, $C_2H_5C(O)OO$, and $C_2H_5C(O)O$ are −66.5, −43.2, and −46.6 kcal mol^{-1}, respectively. Dissociation enthalpies of 31.5 and 37.5 kcal mol^{-1} have been predicted for the $C_2H_5C(O)OO$–NO_2 and $C_2H_5C(O)O$–ONO_2 bonds from the above enthalpies of formation. For comparative purposes, results derived from similar calculations are also reported for the peroxyacetyl nitrate, $CH_3C(O)OONO_2$ (PAN) and for the $CH_3C(O)OO$ and $CH_3C(O)O$ radicals.

Keywords: PPN; Potential energy barriers; Enthalpies of formation; *Ab initio*; Density functional theory

1. Introduction

Peroxynitrates, $ROONO_2$, are formed during the photochemical oxidation of non-methane hydrocarbons in the presence of nitrogen oxides, NO_x, and its reactions play crucial roles in the catalytic cycles of NO_x [1–4]. The two major peroxynitrates are peroxyacetyl nitrate, $CH_3C(O)OONO_2$ (PAN), and peroxypropionyl nitrate, $C_2H_5C(O)OONO_2$ (PPN). The first originates from almost all non-methane hydrocarbon species, whereas the second arises mainly from longer chain anthropogenic hydrocarbons like alkanes and alkenes [5]. An important aspect of peroxynitrates is their role in the budget and transport of reactive nitrogen species in the atmosphere. These compounds often constitute a major fraction of the available reactive odd nitrogen. Furthermore, lifetimes of peroxynitrates range from less than an hour at 300 K or higher temperatures, to months at characteristic temperatures of the upper troposphere [6,7]. Thus, they can be transported over long distances from polluted continental regions into the remote troposphere. Therefore, peroxynitrates act as a temporary reservoir for NO_x.

PAN was first identified in urban smog atmosphere by Stephens and co-workers in the 1950s [1] and, at present, is the most well-known member of this class. The formation, global distribution, and thermal chemistry of PAN have been the subject of numerous studies [6,8–18]. Also its spectroscopic and photochemical properties have been well characterized [5,19–22].

The characterization of the thermal decomposition and physicochemical properties for PPN has received much less attention than PAN in the literature. PPN has been measured in ambient air of urban areas and it has been

* Corresponding author. Tel.: +54 221 4257430; fax: +54 221 4254642.
E-mail address: mbadenes@inifta.unlp.edu.ar (M.P. Badenes).

0166-1280/$ - see front matter © 2008 Elsevier B.V. All rights reserved.
doi:10.1016/j.theochem.2008.01.015

assumed that this compound originates only from the oxidation of anthropogenic hydrocarbons [23]. The unimolecular decomposition rate constant of PPN has been studied as a function of temperature and total pressure and its lifetime has been estimated [6].

In this work, we reported an *ab initio* and DFT study of the molecular structures, conformational mobilities and thermochemistry of the PPN and its radical decomposition products $C_2H_5C(O)OO$ and $C_2H_5C(O)O$.

2. Computational methods

All of the density functional and *ab initio* calculations were performed with the Gaussian 03 program package [24]. The methodology employed is similar to that used in a recent publication [25]. The potentials for the internal rotations of PPN, $C_2H_5C(O)OO$, and $C_2H_5C(O)O$ were computed at the B3LYP level of theory using the 6-311++G(d,p) triple split valence basis set [26]. The B3LYP method employs the Becke's three-parameter non-local exchange functional [27,28] coupled to the non-local correlational functional of Lee, Yang, and Parr [29]. The conformational structures of PPN, $C_2H_5C(O)OO$, and $C_2H_5C(O)O$ were fully optimized using analytical gradient methods at the B3LYP/6-311++G(d,p) level of theory. Harmonic vibration frequencies and zero-point vibrational energies (ZPE) were derived at the same level employing analytical second order derivative methods. The fully optimized geometries and harmonic vibrational frequencies for the most stable conformations and transition structures between rotational conformers were calculated at the B3LYP/6-311++G(3df,3pd) level of theory. The diffuse functions included in the basis set grant radial flexibility to represent electron density far from the nuclei, while the p, d, and f-type polarization functions confer angular flexibility to represent regions of high electron density among the bonded atoms. In addition, we have also used the G3MP2B3 model chemistry [30] and a modified version that employs for the molecular geometries and vibrational frequencies the functional B3LYP/6-311++G(3df,3pd) instead of standard B3LYP/6-31G(d) [31–34]. This approach is denoted here as G3MP2//B3LYP/6-311++G(3df,3pd). The G3MP2B3 model uses a reduced order of perturbational theory and only valence electrons in the treatment of the correlation energy. Under certain assumptions about additivity [30,35], the final total energies are comparable to those calculated at the QCISD(T, full)/G3Large level. The average absolute deviation from well-known experimental enthalpies of formation is 1.13 kcal mol^{-1} for the G3MP3B3 model [30].

3. Results and discussion

3.1. Torsional barriers

As other peroxynitrates, PPN presents internal rotations around the C—O, O—N, and O—O bonds [25]. Furthermore, PPN also possesses two rotations around its two C—C bonds. Potential barriers for all internal rotations were individually calculated to investigate the hindered degree of the rotational conformers. For this, we have computed the total energy as a function of the dihedral angles by scanning the torsion angles between 0° and 360° in steps of 20°, while all remaining coordinates were fully optimized at the B3LYP/6-311++G(d,p) level of theory. Then, the total energy corresponding to the most stable molecular conformer was arbitrarily set to zero and thus used as a reference point to calculate the potential barriers. In addition, the geometries at the critical points were fully optimized at the same level. The molecular structures of the different rotational conformers (minima of potential energy curve) and transition states (maxima of potential energy curve) of PPN are depicted in Fig. 1, and the resulting potential barriers for all internal rotations are shown in Figs. 2–4.

The calculated rotational potentials were fitted to a truncated Fourier expansion,

$$V(\Phi) = a_0 + \sum a_i \cos(i\Phi) + \sum b_i \sin(i\Phi) \quad \text{(I)}$$

where $V(\Phi)$ is the relative energy at torsional angle Φ and $i = 1$–4. For all cases, values for the squared correlation coefficients r^2 better than 0.9990 were obtained. The resulting coefficients a_i and b_i in Eq. (I) are listed in Table 1.

Fig. 2a shows the calculated rotational barriers around the C—O bond of PPN. This potential presents two minima separated by two barriers of, on average, 12.4 kcal mol^{-1} high at G3MP2B3 level of theory. The imaginary vibrational frequency for these transition states is $\nu = 83$i cm^{-1}. The minima possess a difference of energy of 3.3 kcal mol^{-1} at the same level. The global minimum corresponds to a structure with a C=O bond *syn*- regarding the O—O bond, and a CC—OO dihedral angle of almost 180° (conformer 1). Another minimum, with CC—OO dihedral angle near 0°, corresponds to the *anti*-conformer (conformer 2). For rotation around the O—N bond, we found the calculated symmetric potential energy curve of Fig. 2b. Rotational barriers of 10.7 kcal mol^{-1} ($\nu = 90$i cm^{-1}) were computed at G3MP3B3 level and the two minima resulted equivalent to conformer 1. This is because of rotating group, NO_2, possesses an axis of symmetry and its rotation does not lead to different conformers. The calculated rotational barriers around the C1—C2 bond are shown in Fig. 2c. In this case a rotation of the symmetrical CH_3 group occurs, and the potential curve exhibits three regular minima (1′) and three regular maxima (TS 1′–1′) as normally shows this type of rotations [36,37]. Minima are separated by barriers of 3.0 kcal mol^{-1} ($\nu = 209$i cm^{-1}) at the G3MP2B3 level. Fig. 3a shows the other C—C rotation. It presents only one minimum and one maximum. These points correspond to the conformer 1 and a structure that possesses the CH_3 and the voluminous $OONO_2$ group in the same side (TS), respectively. Furthermore, the calculated barrier of 1.5 kcal mol^{-1} ($\nu = 39$i cm^{-1}) is in the typical range for this kind of rotations [36,37]. Fig. 4 shows the potential energy

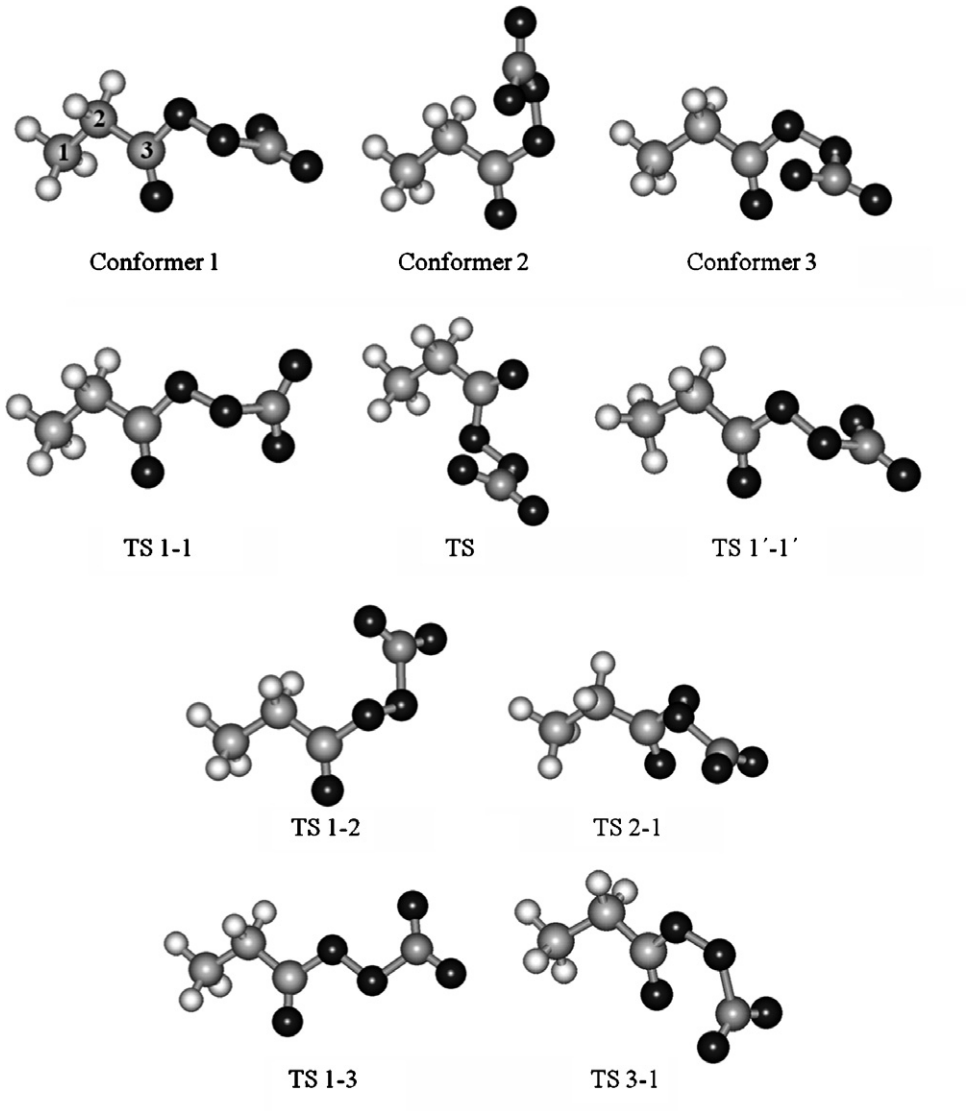

Fig. 1. Molecular structures of different conformers and transition states in PPN optimized at the B3LYP/6-311++G(d,p) level of theory.

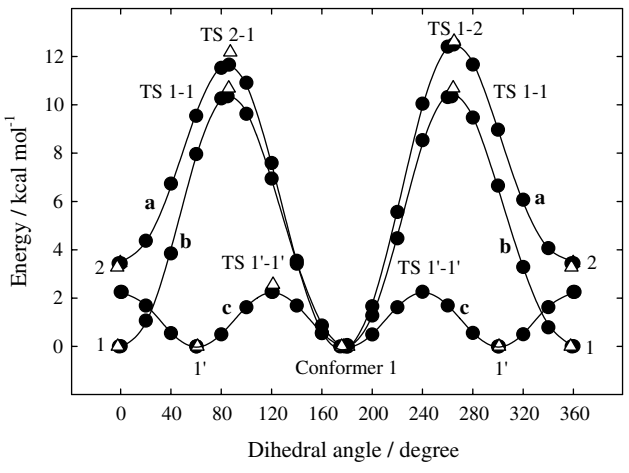

Fig. 2. Potential energy barriers for internal rotation around CC—OO (a), OO—NO (b), and HC1—C2H (c) bonds in PPN. (●) Calculated at the B3LYP/6-311++G(d,p) level; (Δ) calculated at the G3MP2B3 level; (—) Fourier analysis with the coefficient of Table 1.

barriers for internal rotation around O—O bond. This curve presents two minima and two maxima. In this case, the minima correspond to conformer 1 and its optical isomer and two different barriers separate them. The highest barrier of 15.6 kcal mol^{-1} ($v = 192$i cm^{-1}) at a dihedral angle of 0° and the lowest barrier of 5.6 kcal mol^{-1} ($v = 57$i cm^{-1}) at 180° are observed. In all cases, a good agreement between the calculated energies of maxima and minima at the B3LYP/3-11++G(d,p) and G3MP2B3 levels of theory is observed. However, the G3MP2B3 barriers are, in general, 0.4 kcal mol^{-1} higher.

Subsequently, we analyzed the possibility of obtaining new conformers from the O—O rotation of conformer 2. Nevertheless, this rotation only leads to an optical isomer of conformer 2. In summary, PPN exhibits two rotational conformers: *syn*-PPN (conformer 1) and *anti*-PPN (conformer 2), and the *syn*-form is predicted to be favoured.

In a similar way, we studied the internal rotations in $C_2H_5C(O)OO$ and $C_2H_5C(O)O$ radicals. The

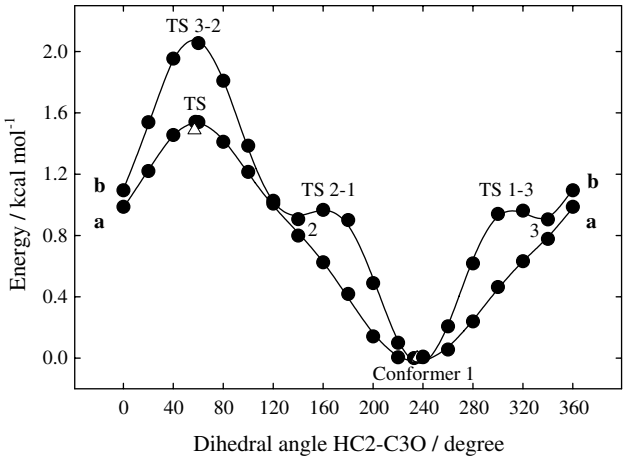

Fig. 3. Potential energy barriers for internal rotation around HC2—C3O bond in PPN (a) and $C_2H_5C(O)OO$ (b). (●) Calculated at the B3LYP/6-311++G(d,p) level; (Δ) calculated at the G3MP2B3 level; (—) Fourier analysis with the coefficient of Table 1 for PPN and Table 2 for $C_2H_5C(O)OO$.

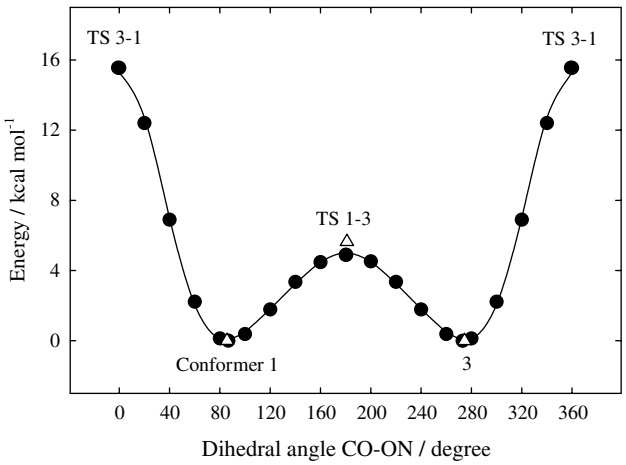

Fig. 4. Potential energy barriers for internal rotation around CO—ON bond in PPN. (●) Calculated at the B3LYP/6-311++G(d,p) level; (Δ) calculated at the G3MP2B3 level; (—) Fourier analysis with the coefficient of Table 1.

$C_2H_5C(O)OO$ presents two rotations around C—C bonds and one around C—O bond, while the $C_2H_5C(O)O$ exhibits only two rotations about C—C bonds. As for PPN, the calculated rotational potentials have been fitted employing truncated Fourier series and the values for the coefficients are listed in Table 2. The $C_2H_5C(O)OO$ and $C_2H_5C(O)O$ potential energy curves present characteristics similar to found for PPN. As an example, Fig. 6a shows that rotation about C1—C2 bond in $C_2H_5C(O)OO$ leads to three regular minima and maxima as in PPN. Moreover, this potential fits almost perfectly with the corresponding potential of PPN. The same occurs with the other C—C rotation (Fig. 3b). Nevertheless, in the case of $C_2H_5C(O)OO$ radical, it is possible to distinguish local maxima and minima in the potential. More precisely, the potential presents one barrier of 2.1 kcal mol^{-1} ($v = 46$i cm^{-1}) and two small barriers of 1.0 kcal mol^{-1} ($v = 32$i cm^{-1}) at the G3MP2B3 level. These barriers connect the conformers 1, 2, and 3 of $C_2H_5C(O)OO$. The rotation around C—O bond (Fig. 6b) presents two barriers of 5.2 kcal mol^{-1} ($v = 114$i cm^{-1}), which are approximately 50% smaller than those in PPN. This probably occurs because of the larger C—O bond length and the lower rotating group volume in the radical. In this case, the minima correspond to conformers *syn*-$C_2H_5C(O)OO$ (conformer 1) and *anti*-$C_2H_5C(O)OO$ (conformer 4), with energies that differ only by 0.2 kcal mol^{-1}. All rotamers are displayed in Fig. 5. Rotations about the C—C bonds of $C_2H_5C(O)O$ do not cause different conformers, as Fig. 7 shows, due to the fact that the rotating groups, CH_3 and CO_2, possess an axis of symmetry. Rotation about C1—C2 bond (Fig. 7a) presents three regular minima connected by barriers of 2.4 kcal mol^{-1} ($v = 205$i cm^{-1}) at the G3MP2B3 level, that is approximately 0.6 kcal mol^{-1} lower than the value for PPN. On the other hand, the symmetric rotational potential around C2—C3 bond shows two minima and maxima (Fig. 7b). For this case, small rotational barriers of 0.5 kcal mol^{-1} ($v = 40$i cm^{-1}) were calculated at the same level. In summary, we found four rotamers for $C_2H_5C(O)OO$ radical, being the most stable conformer 4, and only one conformation for $C_2H_5C(O)O$ radical (Fig. 5). The standard enthalpy of formation for rotamers of PPN and $C_2H_5C(O)OO$ is discussed in Section 3.4.

Practically identical potential barriers were observed for the common internal rotations of PPN and PAN. In fact, employing the a_i and b_i coefficients listed in Table 1 the

Table 1
Coefficients of the Fourier expansion for torsional potentials of PPN and PAN (in brackets) calculated at the B3LYP/6-311++G(d,p) level of theory

Coefficient (kcal mol^{-1})	Rotations				
	C(1)—C(2)	C(2)—C(3)	O—O	O—N	C—O
a_0	1.102	0.722	4.668 (4.648)	4.943 (4.963)	6.587 (6.739)
a_1	2.45×10^{-3}	0.364	3.508 (3.543)	−0.152 (−0.148)	1.392 (1.302)
a_2	6.46×10^{-4}	−0.025	5.025 (4.959)	−5.178 (−5.162)	−5.157 (−5.363)
a_3	1.132	−0.070	1.628 (1.611)	0.145 (0.140)	0.413 (0.475)
a_4	2.04×10^{-3}	−0.011	0.455 (0.422)	0.207 (0.171)	0.264 (0.284)
b_1	-1.84×10^{-3}	0.606	-1.42×10^{-3} (−0.015)	−0.049 (−0.049)	−0.495 (−0.476)
b_2	-1.12×10^{-3}	8.36×10^{-3}	3.01×10^{-3} (−0.032)	0.548 (0.616)	0.752 (0.754)
b_3	0.035	0.020	-3.96×10^{-3} (1.6×10^{-3})	−0.058 (−0.053)	−0.063 (−0.069)
b_4	-4.74×10^{-4}	−0.012	4.42×10^{-3} (0.035)	−0.251 (−0.257)	−0.127 (−0.124)

Table 2
Coefficients of the Fourier expansion for torsional potentials of $C_2H_5C(O)OO$ and $C_2H_5C(O)O$ calculated at the B3LYP/6-311++G(d,p) level of theory

Coefficient (kcal mol^{-1})	Rotations				
	$C_2H_5C(O)OO$			$C_2H_5C(O)O$	
	C(1)—C(2)	C(2)—C(3)	C—O	C(1)—C(2)	C(2)—C(3)
a_0	1.110	0.992	2.527	1.016	0.194
a_1	2.979×10^{-3}	0.412	−0.303	2.504×10^{-4}	-7.415×10^{-4}
a_2	9.377×10^{-4}	−0.015	−2.666	1.527×10^{-3}	−0.201
a_3	1.127	−0.295	0.298	1.046	1.621×10^{-3}
a_4	1.499×10^{-3}	5.324×10^{-3}	0.030	2.345×10^{-3}	-2.659×10^{-3}
b_1	-2.917×10^{-3}	0.636	-1.713×10^{-5}	2.845×10^{-3}	-3.959×10^{-5}
b_2	4.160×10^{-4}	0.041	-2.388×10^{-5}	-5.126×10^{-4}	1.370×10^{-4}
b_3	0.066	0.052	-3.852×10^{-5}	0.046	3.241×10^{-4}
b_4	1.362×10^{-4}	0.014	7.190×10^{-6}	-3.420×10^{-4}	2.898×10^{-4}

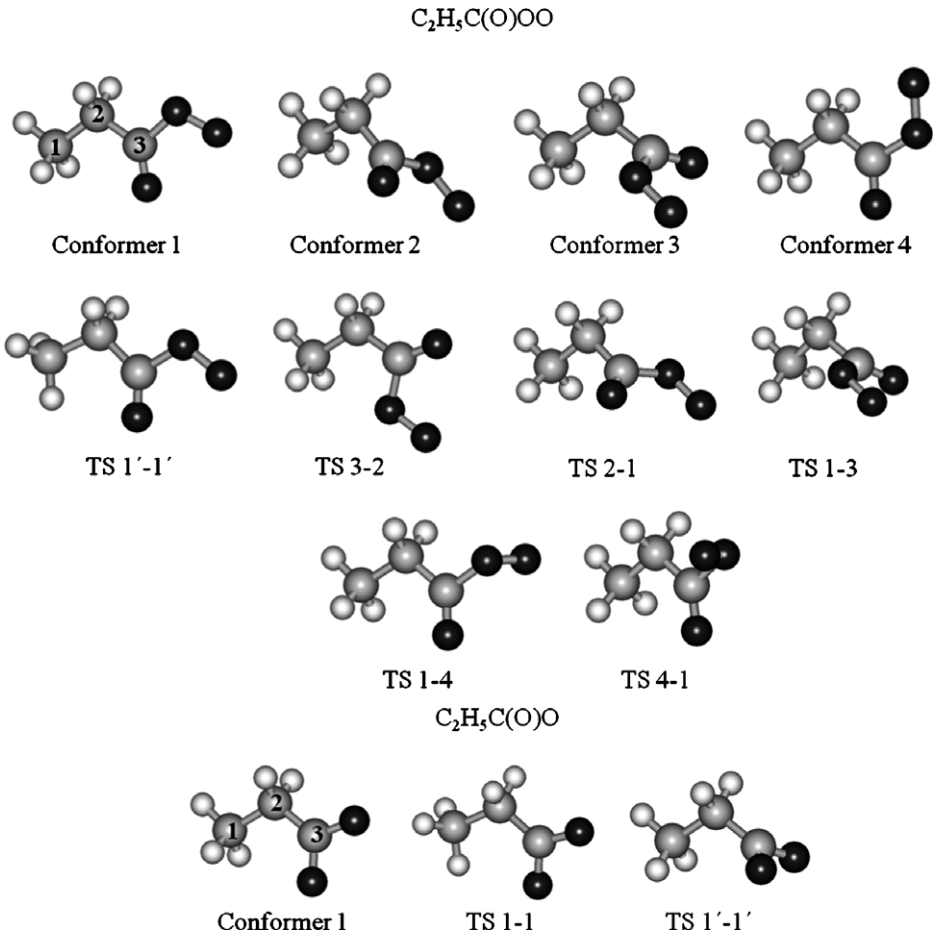

Fig. 5. Molecular structures of different conformers and transition states in $C_2H_5C(O)OO$ and $C_2H_5C(O)O$ optimized at the B3LYP/6-311++G(d,p) level of theory.

rotational potential for PAN can be easily constructed. To our knowledge, no rotational barriers have been reported so far for both PPN and PAN.

3.2. Molecular structures and harmonic vibrational frequencies

To investigate the structural properties and harmonic vibrational frequencies of the most stable conformers of PPN and PAN we have performed calculations at the B3LYP/6-311++G(3df,3pd) level of theory. At this level, the frequency scaled factor is expected to be close to unity [38].

The computed geometrical parameters and harmonic vibrational frequencies obtained for PAN agree very satisfactorily with those derived at different levels of theory [15,39]. In fact, the small mean absolute deviations of 0.003 Å for the bond distances and 0.2° for the bond angles

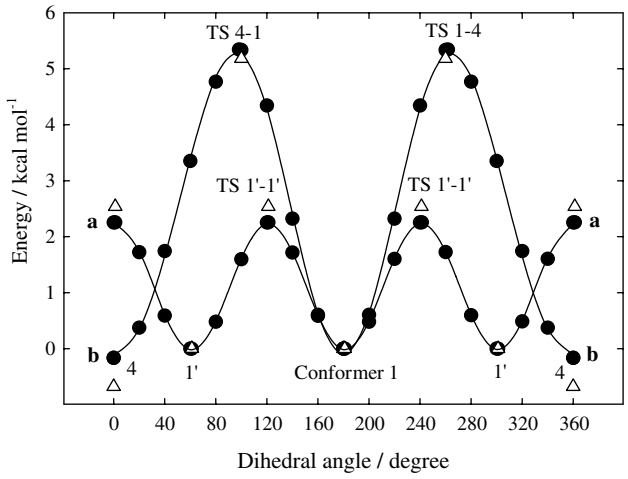

Fig. 6. Potential energy barriers for internal rotation around HC1—C2H (a), and CC—OO (b) bonds in $C_2H_5C(O)OO$. (●) Calculated at the B3LYP/6-311++G(d,p) level; (Δ) calculated at the G3MP2B3 level; (—) Fourier analysis with the coefficient of Table 2.

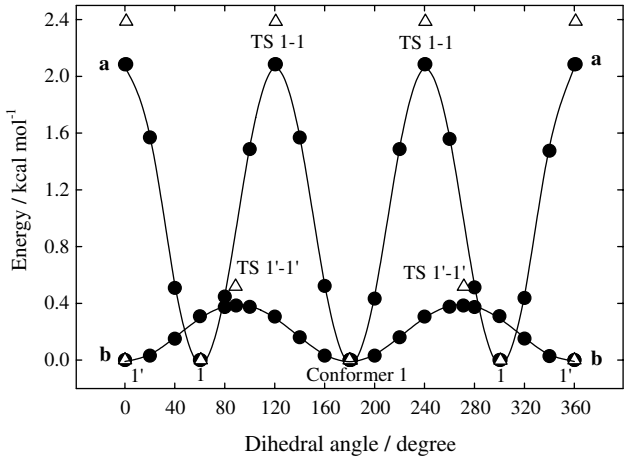

Fig. 7. Potential energy barriers for internal rotation around HC1—C2H (a) and CC2—C3O (b) bonds in $C_2H_5C(O)O$. (●) Calculated at the B3LYP/6-311++G(d,p) level; (Δ) calculated at the G3MP2B3 level; (—) Fourier analysis with the coefficient of Table 2.

indicate very good agreement found. Furthermore, a comparison between calculated and experimental vibrational frequencies led to mean deviations of 66 cm^{-1}. In the context of this work, PAN mainly served as a test case for used method. That is, the obtained results point out that the B3LYP/6-311++G(3df,3pd) method should provide an accurate representation of the structural parameters and vibrational frequencies of PPN.

The computed geometrical parameters of PPN are listed in Table 3. As it occurs in other peroxynitrates, PPN possesses two approximately plane groups, CCC(O)O and $OONO_2$. However, in this case, the hydrogen atoms of the carbonated group go out of the plane formed for CCC(O)O atoms. The calculated dihedral angle between these two planes, $\tau(COON) = 85.9°$, agrees very well with dihedral angles observed in other peroxynitrates with two sp^2-hybridized groups (RC(O) and NO_2) [25,39,40]. The calculated O—O bond length of 1.399 Å coincides exactly with the same bond length in PAN and is slightly shorter than those observed in other acylperoxynitrates [25,39,40]. The same occurs with the O—N bond length of 1.511 Å.

Computed harmonic vibrational frequencies, infrared intensities and approximate mode assignations along with available experimental data for PPN, $C_2H_5C(O)OO$, and $C_2H_5C(O)O$ are given in Table 4. For PPN, a comparison between calculated and experimental data leads to mean absolute deviations of 41 cm^{-1}. Mode assignations were derived from the animation of the normal modes corresponding to the fundamental vibrational frequencies and by a comparison with the spectra of other peroxynitrates. Most of the modes are appreciably mixed and therefore the consigned assignations are approximate. In fact, only the stretching movements at high wave numbers and torsions at small wave numbers are almost decoupled from the rest of the modes. For example, frequencies of about 3000 cm^{-1} correspond to stretching movements and those at around 1450 cm^{-1} to deformations of CH_3 group, as it occurs in PAN [15]. Moreover, stretching NO_2, C═O, C—O, O—O, and O—N groups occur at similar wave number that analogous motions in PAN [15], $FC(O)OONO_2$ [40], and $CF_3C(O)OONO_2$ [41]. In summary, PPN possesses 36 vibrational frequencies divided in thirteen stretching, eighteen deformations or bending and five torsions. In the cases of $C_2H_5C(O)OO$ and $C_2H_5C(O)O$ radicals, the computed vibrational frequencies are similar to the corresponding for PPN.

3.3. Population of molecules with free internal rotations

To analyze if rotations of the molecular moieties are free, partially or totally hindered at room temperature, we estimate the population of molecules with free internal rotation about a particular bond. We performed these calculations from information obtained of rotational potentials and computed vibrational frequencies. It is also necessary to know the partition function of each internal rotation. To calculate the partition function for a hindered internal rotor we have employed the expression (II) proposed by Troe [42],

$$Q_{\text{rot int}} \approx Q_{\text{tors}}[\exp(-RT/V_0)]^{1.2} + Q_{\text{free}}[1 - \exp(-RT/V_0)]^{1.2} \quad \text{(II)}$$

In the above expression, V_0 is the barrier high, Q_{tors} and Q_{free} are partition functions calculated with internal rotations considered as totally restricted (torsions) and as completely free, respectively. These partition functions were estimated by using the well-known statistical formulae (III) and (IV)

$$Q_{\text{tors}} = [1 - \exp(-\hbar\nu_{\text{tors}}/RT)]^{-1} \quad \text{(III)}$$

$$Q_{\text{free}} = (2\pi I_{\text{m}} kT/\hbar^2)^{1/2} \quad \text{(IV)}$$

Table 3
Geometrical parameters of *syn*-$C_2H_5C(O)OONO_2$, *anti*-$C_2H_5C(O)OO$, and $C_2H_5C(O)O$ calculated at the B3LYP/6-311++G(3df,3pd) level of theory (bond lengths in Ångstroms and angles in degrees)

Parameter	*syn*-$C_2H_5C(O)OONO_2$	*anti*-$C_2H_5C(O)OO$	$C_2H_5C(O)O$
r(C═O)	1.187	1.179	1.252
r(N═O)$_{mean}$	1.186	–	–
r(C1—C2)	1.524	1.524	1.527
r(C2—C3)	1.506	1.499	1.496
r(O—C)	1.404	1.454	1.259
r(O—N)	1.511	–	–
r(O—O)	1.399	1.315	–
r(C—H)$_{mean}$ in CH_2	1.092	1.093	1.093
r(C—H)$_{mean}$ in CH_3	1.088	1.089	1.089
∠(O═CC)	129.0	130.3	125.0
∠(OCC)	107.8	107.7	123.8
∠(OOC)	111.9	113.5	–
∠(OON)	109.6	–	–
∠(O═N═O)	133.9	–	–
DIH(COON)	85.9	–	–

Table 4
Harmonic vibrational frequencies (in cm^{-1}), approximated assignations and infrared intensities (in km mol^{-1}) for *syn*-$C_2H_5C(O)OONO_2$, *anti*-$C_2H_5C(O)OO$, and $C_2H_5C(O)O$ calculated at the B3LYP/6-311++G(3df,3pd) level of theory

Assignation	*syn*-$C_2H_5C(O)OONO_2$		*anti*-$C_2H_5C(O)OO$	$C_2H_5C(O)O$
	Experimental[a]	Calculated		
Str sym CH_3	2996.4	3123 (15)	3120 (15)	3118 (15)
Str sym CH_2	–	3118 (14)	3118 (14)	3115 (11)
Str asym CH_3	–	3074 (1)	3065 (0.8)	3071 (1)
Str asym CH_3	2960.5	3050 (20)	3050 (17)	3048 (13)
Str asym CH_2	–	3046 (5)	3039 (7)	3041 (4)
Str asym NO_2	1833.7	1876 (184)	–	1585 (165)[b]
Str C═O	1738.5	1804 (427)	1911 (192)	1503 (2)[c]
Str sym NO_2	–	1504 (9)	–	–
Bend CH_2	–	1497 (8)	1497 (8)	1423 (6)
Def asym CH_3	1467.2	1460 (17)	1503 (8)	1497 (8)
Def asym CH_3	1432.4	1426 (3)	1455 (19)	1454 (25)
Bend CH_2	–	1375 (13)	1427 (3)	1348 (13)
Str C(2)—C(3)	1437.3	1350 (248)	1376 (14)	1285 (0.3)
Str C—O	1299.7	1286 (0.1)	800 (11)	–
Str C(1)—C(2)	1156.2	1117 (81)	1281 (0.2)	1109 (1)
Wag CH_2	1097.0	1112 (4)	1166 (10)	1150 (71)
Rock CH_3	1042.9	1048 (117)	1105 (44)	1069 (3)
Wag CH_2	990.1	1003 (112)	768 (101)	1002 (0.3)
Rock CH_3	963.1	973 (7)	1102 (0.4)	804 (12)
Str O—O	920.6	854 (48)	974 (88)	–
Rock CH_3	851.1	813 (140)	1037 (74)	–
Bend COO	–	808 (67)	–	–
Out of plane N	793.1	735 (8)	–	–
Bend NO_2	–	711 (4)	–	–
Out of plane C(2)	–	643 (13)	–	–
Out of plane C(3)	582	562 (5)	526 (3)	531 (5)
Str N—O	–	512 (35)	–	–
Bend CCCH	–	370 (3)	422 (10)	844 (14)
Bend ONO	–	348 (9)	–	–
Out of plane O(3)	–	322 (4)	–	–
Out of plane O(2)	–	220 (1)	–	–
Torsion O—O	–	209 (1)	–	–
Torsion N—O	–	99 (0.4)	–	–
Torsion C—O	–	76 (0.1)	207 (1)	–
Torsion C(2)—C(3)	–	70 (2)	119 (0.01)	193 (1)
Torsion C(1)—C(2)	–	23 (0.3)	56 (1)	35 (1)

[a] Reference [6].
[b] Str sym CO_2.
[c] Str asym CO_2.

Here, v_{tors} is the torsional frequency and $I_m = I_A I_B/(I_A + I_B)$ is the reduced moment of inertia for the selected rotation. Then, the percentage of molecules with free internal rotation around a given bond is

$$R_{free} = \{100\, Q_{free}[1 - \exp(-RT/V_0)]^{1,2}\}/Q_{rot\ int} \quad (V)$$

For V_0 and v_{tors}, we have used the values derived from G3MP2B3 and B3LYP/6-311++G(3df,3pd) calculations, respectively. To estimate I_m values, we assumed that the molecule is formed by a pair of symmetrical coaxial tops A and B with moment of inertia I_A and I_B, and we have employed the geometrical parameters obtained at the B3LYP/6-311++G(3df,3pd) level. The used molecular input data, internal rotational partition functions and calculated R_{free} values at 298 K, are listed in Table 5. As the results show, all rotations in PPN are practically restricted. Own of the low rotational barrier of 1.5 kcal mol^{-1}, about 20% of the C_2H_5 and $C(O)OONO_2$ moieties can rotate freely around the C_2H_5—$C(O)OONO_2$ bond. This value is somewhat larger to the recently estimated for the same bond in CH_2 =CHC(O)OONO$_2$ (APAN) of 8% [25]. On the other hand, the R_{free} values calculated for the C—O, O—N and O—O bonds in APAN of 6%, 8%, and 5% are comparable with the here estimated for PPN.

3.4. Thermochemistry

The methodology employed to estimate the enthalpies of formation of PPN, $C_2H_5C(O)OO$, and $C_2H_5C(O)O$ is similar to that used in recent publications from this laboratory [25,31–34,43]. They were computed from total atomization energies and from isodesmic reaction schemes. In the first approach, we estimate the total atomization energy, $\sum D_0$, by subtracting of the computed energy of the molecule from of those of the component atoms at 0 K. Then the enthalpies of formation at 0 K, $\Delta H_{f,0}$, can be calculated by subtracting the computed total atomization energy from the experimental enthalpies of formation of carbon (169.98 ± 0.1 kcal mol^{-1}), hydrogen (51.63 ± 0.001 kcal mol^{-1}), nitrogen (112.53 ± 0.02 kcal mol^{-1}), and oxygen atoms (58.99 ± 0.02 kcal mol^{-1}) [44]. The enthalpies of formation derived in this way were afterwards transformed to 298 K, $\Delta H_{f,298}$, using estimated thermal contributions and $H°_{298\ K} - H°_{0\ K}$ values for carbon, hydrogen, nitrogen, and oxygen atoms of 0.25, 1.01, 1.04, and 1.04 kcal mol^{-1} [45]. The resulting $\sum D_0$ and $\Delta H_{f,298}$ for PPN, $C_2H_5C(O)OO$, and $C_2H_5C(O)O$ are listed in Table 6. A comparison between the enthalpies of formation obtained at different levels of theory indicates that, as expected, the B3LYP model with the smallest basis set used provides very poor results. This deficiency is corrected by using a much larger basis set. In fact, the B3LYP model with the highest basis set employed, 6-311++G(3df,3pd), leads to enthalpies of formation for PPN, $C_2H_5C(O)OO$, and $C_2H_5C(O)O$ very close to those evaluated with the more accurate G3MP2B3 and G3MP2//B3LYP/6-311++G (3df,3pd) models.

The second useful alternative, the computation of isodesmic and isogyric reactions energies, usually leads to more reliable enthalpies of formation.

As a consequence, systematic errors due to incompleteness of the basis sets and electron correlation energy cancel to a great extension [46]. In this procedure, the enthalpy of formation for a given compound is calculated by coupling the *ab initio* theoretically computed enthalpy change of a selected isodesmic reaction, ΔHr, with well-known enthalpies of formation for other reaction components. For this, the isodesmic reactions given in Table 7 were considered. All energy calculations were carried out on optimized geometries computed at B3LYP level. As before, obtained results for PAN suggest that this level of theory is suitable to predict the energetic of PPN. In fact, our best estimation of −61.0 kcal mol^{-1} obtained for enthalpy of formation of PAN agrees very well with the value of −61.2 ± 5.3 kcal mol^{-1} derived by Bridier and co-workers from the experimental dissociation enthalpy of PAN into $CH_3C(O)OO$ and NO_2 radicals [13]. All reaction enthalpies listed in Table 7 were corrected by ZPE and thermal contributions to the internal energy of the compounds (298 K, 1 atm). To determine the $\Delta H_{f,298}$ values, the well-established experimental enthalpies of formation listed in Table 8 are required. As expected, no large basis set effects are observed. Moreover, the pronounced difference found between the $\Delta H_{f,298}$ values computed from $\sum D_0$ at B3LYP level with the two basis set employed, is notably diminished by using isodesmic reactions. This improvement is mostly ascribed to compensation effects, which reduce the importance of the truncation in the one-electron basis set. On the other hand, the values obtained from the more reliable Gaussian-3 theory, result more negative than those derived from B3LYP method. Calculations with energies computed at the G3MP2//B3LYP/6-311++G (3df,3pd) level of theory yielded our best values of −66.5 ± 2, −43.2 ± 2, and −46.6 ± 2 kcal mol^{-1} for enthalpies of formation of PPN, $C_2H_5C(O)OO$, and $C_2H_5C(O)O$, respectively. The assigned errors are based on the dispersion of the calculated values listed in Table 7 and on the uncertainties of the experimental enthalpies of formation of Table 8.

Table 5
Employed molecular input data, internal rotational partition functions, and calculated percentages of molecules with free internal rotations at 298 K for *syn*-$C_2H_5C(O)OONO_2$

Property	Internal rotation				
	C(1)—C(2)	C(2)—C(3)	C—O	O—N	O—O
V_0 (kcal mol^{-1})	2.6	1.5	12.6	10.7	15.6
v_{tors} (cm^{-1})	23	70	76	99	209
I_m (amu Å^2)	3.0	4.8	53.8	33.4	21.5
Q_{free}	10.8	13.6	45.6	35.9	28.8
Q_{tors}	57.1	19.1	17.6	13.7	6.7
$Q_{rot.\ int.}$	45.0	15.4	17.8	13.9	7.0
R_{free} (%)	4	23	6	8	8

Table 6
Calculated atomization energies and enthalpies of formation for *syn*-$C_2H_5C(O)OONO_2$ (PPN), *anti*-$C_2H_5C(O)OO$, and $C_2H_5C(O)O$ (in kcal mol^{-1})

Level of theory	PPN		$C_2H_5C(O)OO$		$C_2H_5C(O)O$	
	$\sum D_0$	$\Delta H_{f,298}$	$\sum D_0$	$\Delta H_{f,298}$	$\sum D_0$	$\Delta H_{f,298}$
B3LYP/6-311++G(d,p)	1210.8	−40.7	969.8	−28.7	923.2	−40.9
B3LYP/6-311++G(3df,3pd)	1232.6	−62.6	982.5	−41.5	933.1	−50.8
G3MP2B3	1233.7	−63.6	981.6	−41.1	932.8	−50.4
G3MP2//B3LYP/6-311++G(3df,3pd)	1231.7	−61.7	982.1	−41.1	928.4	−46.1

Table 7
Isodesmic reactions, calculated enthalpy changes and enthalpies of formation (in kcal mol^{-1}) for *syn*-$C_2H_5C(O)OONO_2$ (PPN), *anti*-$C_2H_5C(O)OO$, $C_2H_5C(O)O$, *syn*-$CH_3C(O)OONO_2$ (PAN), *anti*-$CH_3C(O)OO$, and $CH_3C(O)O$

Isodesmic reaction	B3LYP/BS1		B3LYP/BS2		G3MP2B3		G3MP2//B3LYP/BS2	
	ΔH_r	$\Delta H_{f,298}$	ΔH_r	$\Delta H_{f,298}$	ΔH_r	$\Delta H_{f,298}$	ΔH_r	$\Delta H_{f,298}$
syn-$C_2H_5C(O)OONO_2$ (PPN)								
$HNO_3 + C_2H_6 + CH_3C(O)OH + H_2O_2 \rightarrow PPN + 2\ H_2O + CH_4$	−6.1	−60.6	−6.6	−61.1	−11.0	−65.5	−11.1	−65.6
$HNO_3 + 2\ C_2H_6 + H_2CO + CH_3O_2H \rightarrow PPN + H_2O + 3\ CH_4$	−42.6	−62.7	−43.1	−63.2	−46.3	−66.4	−46.6	−66.7
$HNO_3 + C_2H_6 + CH_3CHO + CH_3O_2H \rightarrow PPN + H_2O + 2\ CH_4$	−31.0	−62.5	−31.4	−62.9	−35.6	−67.1	−35.8	−67.3
		−61.9		−62.4		−66.3		−66.5
anti-$C_2H_5C(O)OO$ (PP)								
$C_2H_6 + CH_3C(O)OH + CH_3O_2 \rightarrow PP + CH_3OH + CH_4$	13.3	−42.2	13.2	−42.3	11.2	−44.3	11.2	−44.3
$2\ C_2H_6 + H_2CO + CH_3OH + HO_2 \rightarrow PP + H_2O + 3\ CH_4$	−39.8	−39.5	−40.1	−39.8	−41.8	−41.5	−42.1	−41.8
$C_2H_6 + CH_3CHO + CH_3O + H_2O_2 \rightarrow PP + H_2O + 2\ CH_4$	−44.6	−39.3	−45.3	−40.0	−49.0	−43.7	−48.8	−43.5
		−40.3		−40.7		−43.2		−43.2
$C_2H_5C(O)O$ (P)								
$C_2H_6 + CH_3C(O)OH + CH_3O_2 \rightarrow P + CH_3O_2H + CH_4$	21.5	−48.8	21.7	−48.6	21.4	−48.9	24.2	−46.1
$2\ C_2H_6 + H_2CO + CH_3O \rightarrow P + 3\ CH_4$	−40.6	−49.2	−41.0	−49.6	−41.4	−50.0	38.4	−47.0
$C_2H_6 + CH_3CHO + CH_3OH + HO_2 \rightarrow P + H_2O_2 + 2\ CH_4$	−12.7	−49.2	−12.4	−48.9	−12.8	−49.3	−10.1	−46.6
		−49.1		−49.0		−49.4		−46.6
syn-$CH_3C(O)OONO_2$ (PAN)								
$HNO_3 + CH_3C(O)OH + H_2O_2 \rightarrow PAN + 2\ H_2O$	−4.2	−56.5	−4.7	−57.0	−7.8	−60.1	−7.8	−60.1
$HNO_3 + C_2H_6 + H_2CO + CH_3O_2H \rightarrow PAN + H_2O + 2\ CH_4$	−40.7	−58.5	−41.2	−59.0	−43.1	−60.9	−43.3	−61.1
$HNO_3 + CH_3CHO + CH_3O_2H \rightarrow PAN + H_2O + CH_4$	−29.1	−58.4	−29.4	−58.7	−32.4	−61.7	−32.5	−61.8
		−57.8		−58.2		−60.9		−61.0
anti-$CH_3C(O)OO$ (PA)								
$CH_3C(O)OH + HO_2 \rightarrow PA + H_2O$	5.7	−36.7	5.1	−37.3	4.1	−38.3	4.9	−37.5
$C_2H_6 + H_2CO + CH_3OH + HO_2 \rightarrow PA + H_2O + 2\ CH_4$	−38.2	−35.6	−38.9	−36.4	−39.4	−36.9	−38.8	−36.3
$CH_3CHO + CH_3\ O_2H + HO_2 \rightarrow PA + H_2O_2 + CH_4$	−19.2	−38.6	−19.7	−39.1	−20.6	−40.0	−19.9	−39.3
		−37.0		−37.6		−38.4		−37.7
$CH_3C(O)O$ (A)								
$CH_3C(O)OH + HO_2 \rightarrow A + H_2O_2$	20.4	−47.3	20.6	−47.1	22.1	−45.6	25.8	−41.9
$C_2H_6 + H_2CO + CH_3O \rightarrow A + 2\ CH_4$	−39.9	−46.2	−40.2	−46.5	−39.2	−45.5	−35.4	−41.7
$CH_3CHO + CH_3OH + OH \rightarrow A + H_2O + CH_4$	−44.2	−47.5	−44.8	−48.1	−41.6	−44.9	−38.1	−41.3
		−47.0		−47.2		−45.3		−41.6

BS1 = 6-311++G(d,p) and BS2 = 6-311++G(3df,3pd).

Table 8
Enthalpies of formation at 298 K [47]

Species	$\Delta H_{f,298}$ (kcal mol^{-1})	Species	$\Delta H_{f,298}$ (kcal mol^{-1})
OH	8.91 ± 0.07	CH_3OO	2.15 ± 1.2
HOO	3.2 ± 0.5	CH_3OH	−48.04 ± 0.14
H_2O	−57.798 ± 0.010	CH_3OOH	−33.2 ± 1.9
H_2O_2	−32.5 ± 0.05	C_2H_6	−20.04 ± 0.07
CH_4	−17.80 ± 0.10	CH_3CHO	−39.7 ± 0.1
H_2CO	−25.98 ± 0.01	$CH_3C(O)OH$	−103.4 ± 0.1
CH_3O	4.1 ± 0.9	HNO_3	−32.0 ± 0.1

After the determination of the enthalpies of formation for PPN, $C_2H_5C(O)OO$, and $C_2H_5C(O)O$, the immediate step is the calculation of the dissociation enthalpies of the O—N and O—O bonds in PPN. These quantities are closely related to the thermal stability of the peroxynitrate. The individual bond dissociation enthalpy values computed from isodesmic enthalpies of formation and by combination of total energies calculated in a direct way are given in Table 9. First calculations were made using the isodesmic enthalpies of formation of PPN, $C_2H_5C(O)OO$, and $C_2H_5C(O)O$ given in Table 7 in conjunction with the values of 8.17 ± 0.1 and 17.6 ± 0.3 kcal mol^{-1} reported for NO_2 and NO_3, respectively [49].

As in the case of APAN, the results emphasize the importance of using a high level of theory to calculate bond dissociation energies [25]. This is more critical when calculations are performed in a direct way. However, when we

Table 9
Calculated $C_2H_5C(O)OO{-}NO_2$ and $C_2H_5C(O)O{-}ONO_2$ bond dissociation enthalpies (in kcal mol^{-1}) at 298 K derived from direct and isodesmic methods

Level of theory	PPN → $C_2H_5C(O)OO + NO_2$		PPN → $C_2H_5C(O)O + NO_3$	
	Direct	Isodesmic	Direct	Isodesmic
B3LYP/6-311++G(d,p)	31.8	29.8	19.5	30.4
B3LYP/6-311++G(3df,3pd)	22.6	29.9	21.1	31.0
G3MP2B3	38.8	31.3	33.1	34.5
G3MP2//B3LYP/6-311++G(3df,3pd)	29.3	31.5	35.8	37.5

use $\Delta H_{f,298}$ derived by isodesmic and isogyric reactions together with other well-established thermodynamic data this problem is largely reduced. The obtained results show that the B3LYP calculations are not very reliable while the G3MP2B3 methods appear to improve the estimations. Moreover, except estimations at the G3MP2//B3LYP/6-311++G(3df,3pd) level, the direct calculations predict that the NO_3 extrusion is more favourable than the NO_2 extrusion. At mentioned model, both direct as isodesmic approaches lead to the conclusion that, as in PAN and APAN [11,17,25,48,49], the O—N bond fission is the more propitious dissociation channel in PPN. At this level of theory, values of 31.5 and 37.5 kcal mol^{-1} are estimated for the O—N and O—O bond dissociation enthalpies, respectively. That is, the difference between both cannels is larger than the same difference for PAN, in which corresponding bond dissociation enthalpies are 28.7 and 30.0 kcal mol^{-1} [47]. Furthermore, the predicted value of 31.5 kcal mol^{-1} compares reasonably well with the activation energy of 27.7 kcal mol^{-1} determined by Kirchner and co-workers for the thermal decomposition of PPN at the high pressure limit [6,50].

3.5. Group additivity values

Group additivity is a straightforward and reasonably accurate calculation method to estimate the thermochemical properties of hydrocarbons and oxygenated hydrocarbons. It is particularly useful for larger molecules where high-level *ab initio* or density functional calculations have high computational cost. A group is defined by Benson as "a polyvalent atom (ligancy $\geqslant 2$) in a molecule together with all of its ligands" [51]. A group is written as $X(A)_i(B)_j(C)_k(D)_l$, where X is the central atom attached to *i* A atoms, *j* B atoms, etc.

In this work, we have calculated group values of $O(O)(NO_2)$ using enthalpies of formation derived for PAN, PPN, and APAN, together with the enthalpies of formation for $HOONO_2$ and CH_3OONO_2 taken from the literature. For this, the enthalpies of formation of each molecule are represented as contributions of groups that constitute it. That is, $\Delta H_f(ROONO_2) = O(R)(O) + O(O)(NO_2)$. For the remaining groups we used the group additivity values (GAV) listed in Table 10. The enthalpies of the $O(O)(NO_2)$ group resulting from data of five peroxynitrates are summarized in Table 11. The mean value for these species is 3.4 kcal mol^{-1}, where the maximum deviation is 1.3 kcal mol^{-1}. The predicted value agrees remarkably well with the value 3.3 ± 3.6 kcal mol^{-1} derived from a set of four peroxynitrates [13] and is slightly higher than the value 2.9 ± 2.2 kcal mol^{-1} obtained using only three molecules [16]. In conclusion, the value estimated here for the enthalpy of the $O(O)(NO_2)$ group is in agreement with other determinations and reduce the literature uncertainties.

Table 10
Group additivity values (GAV) for enthalpies of formation at 298 K [52] (in kcal mol^{-1})

Group	$\Delta H_{f,298}$	Group	$\Delta H_{f,298}$
$C(CO)H_3$	−10.0	O(CO)(O)	−18.2
$C(O)H_3$	−10.0	$C(C)(CO)(H)_2$	−5.2
$C_d(H)_2$	6.3	$C_d(H)(CO)$	5.0
O(H)(O)	−16.3	CO(C)(O)	−35.2
O(C)(O)	−5.0	$CO(C_d)(O)$	−32.2

Table 11
Enthalpy of formation and additivity $O(O)(NO_2)$ group values (in kcal mol^{-1})

R	$\Delta H_{f,298}(ROONO_2)$	GAV[O(O)(NO$_2$)]
H	−12.7[a]	3.6
CH_3	−10.6[b]	4.4
$CH_3C(O)$	−61.0[c]	2.4
$C_2H_5C(O)$	−66.5[c]	2.1
$CH_2{=}CHC(O)$	−34.5[d]	4.4
		3.4

[a] Reference [47].
[b] Reference [53].
[c] This work.
[d] Reference [25].

4. Conclusions

Ab initio calculations have been carried out to study an important member of the acyl peroxynitrates, the peroxypropionyl nitrate (PPN). The torsional potentials and molecular properties of PPN, $C_2H_5C(O)OO$, and $C_2H_5C(O)O$ have been computed using B3LYP and Gaussian-3 model chemistry. First, PAN has been studied to test the used methods, and the data obtained were in excellent agreement with the previous literature data. Then, equilibrium geometries and harmonic vibrational frequencies

along with standard enthalpies of formation for PPN, $C_2H_5C(O)OO$, and $C_2H_5C(O)O$ have been determined. At the best level of theory employed, enthalpy of formation values of −66.5, −43.2, and −46.6 kcal mol^{-1} were calculated for these species. In addition, the O—N and O—O bond dissociation enthalpies were estimated. In this case, the obtained results indicate that PPN is slightly more stable than PAN. Furthermore, the group value of $O(O)(NO_2)$ was derived with the intention of improve the group additivity approach, particularly useful for larger molecules.

Acknowledgements

This research project was supported by the Universidad Nacional de La Plata, the Consejo Nacional de Investigaciones Científicas y Técnicas (CONICET) (PIP 5777), the Comisión de Investigaciones Científicas de la Provincia de Buenos Aires (CICBA), the Agencia Nacional de Promoción Científica y Tecnológica (No. 34499 and No. 38444) and the Max Planck Institute for Biophysical Chemistry Göttingen (Karl Friedrich Bonhoeffer Institute) through the "Partner Group for Chlorofluorocarbons in the Atmosphere".

References

[1] E.R. Stephens, Adv. Environ. Sci. Technol. 1 (1969) 119.
[2] J.M. Roberts, Atmos. Environ. A 24 (1990) 243.
[3] T. Nielsen, U. Samuelsson, P. Grennfelt, E.L. Thomsen, Nature 293 (1981) 553.
[4] H.B. Singh, Environ. Sci. Technol. 21 (1987) 320.
[5] M.H. Harwood, J.M. Roberts, G.J. Frost, A.R. Ravishankara, J.B. Burkholder, J. Phys. Chem. A 107 (2003) 1148.
[6] F. Kirchner, A. Mayer-Figge, F. Zabel, K.H. Becker, J. Chem. Kinet. 31 (1999) 127.
[7] T.J. Wallington, J. Sehested, O.J. Nielsen, Chem. Phys. Lett. 226 (1994) 563.
[8] H.B. Singh, L.J. Salas, W. Viezee, Nature 321 (1986) 588.
[9] B.A. Ridley, J.D. Shetter, B.W. Gandrud, L.J. Salas, H.B. Singh, M.A. Carroll, G. Hubler, D.L. Albritton, D.R. Hastie, H.I. Schi, G.I. Mackay, D.R. Karechi, D.D. Davis, J.D. Bradshaw, M.O. Rodgers, S.T. Sandholm, A.L. Torres, E.P. Condon, G.L. Gregory, S.M. Beck, J. Geophys. Res. 95 (1990) 10179.
[10] S. Seefeld, D.J. Kinnison, J.A. Kerr, J. Phys. Chem. A 101 (1997) 55.
[11] C.E. Miller, J.I. Lynton, D.M. Keevil, J.S. Francisco, J. Phys. Chem. A 103 (1999) 11451.
[12] E.C. Tuazon, W.P.L. Carter, R. Atkinson, J. Phys. Chem. 95 (1991) 2434.
[13] I. Bridier, F. Caralp, H. Loirat, R. Lesclaux, B. Veyret, K.H. Becker, A. Reimer, F. Zabel, J. Phys. Chem. 95 (1991) 3594.
[14] J. Sehested, L.K. Christensen, T. Mogelberg, O.J. Nielsen, T.J. Wallington, A. Guschin, J.J. Orlando, G.S. Tyndall, J. Phys. Chem. A 102 (1998) 1779.
[15] B.J. Mhin, W.Y. Chang, J.Y. Lee, K.S. Kim, J. Phys. Chem. A 104 (2000) 2613.
[16] F. Zabel, Z. Phys. Chem. Bd. 188 (1995) 119.
[17] S. von Ahsen, H. Willner, J.S. Francisco, J. Chem. Phys. 121 (2004) 2048.
[18] R.A. Cox, M.J. Roffey, Environ. Sci. Technol. 11 (1977) 900.
[19] T.L. Mazely, R.R. Friedl, S.P. Sander, J. Phys. Chem. A 101 (1997) 7090.
[20] T.L. Mazely, R.R. Friedl, S.P. Sander, J. Phys. Chem. 99 (1995) 8162.
[21] H.G. Libuda, F. Zabel, Ber. Bunsenges. Phys. Chem. 99 (1995) 1205.
[22] E.L. Varetti, G.C. Pimentel, Spectrochim. Acta A Mol. Biomol. Spectrosc. 30 (1974) 1069.
[23] D. Grosjean, E.L. Williams, E. Grosjean, Environ. Sci. Technol. 27 (1993) 979.
[24] M.J. Frisch, G.W. Trucks, H.B. Schlegel, G.E. Scuseria, M.A. Robb, J.R. Cheeseman, J.A. Montgomery Jr., T. Vreven, K.N. Kudin, J.C. Burant, J.M. Millam, S.S. Iyengar, J. Tomasi, V. Barone, B. Mennucci, M. Cossi, G. Scalmani, N. Rega, G.A. Petersson, H. Nakatsuji, M. Hada, M. Ehara, K. Toyota, R. Fukuda, J. Hasegawa, M. Ishida, T. Nakajima, Y. Honda, O. Kitao, H. Nakai, M. Klene, X. Li, J.E. Knox, H.P. Hratchian, J.B. Cross, C. Adamo, J. Jaramillo, R. Gomperts, R.E. Stratmann, O. Yazyev, A.J. Austin, R. Cammi, C. Pomelli, J.W. Ochterski, P.Y. Ayala, K. Morokuma, G.A. Voth, P. Salvador, J.J. Dannenberg, V.G. Zakrzewski, S. Dapprich, A.D. Daniels, M.C. Strain, O. Farkas, D.K. Malick, A.D. Rabuck, K. Raghavachari, J.B. Foresman, J.V. Ortiz, Q. Cui, A.G. Baboul, S. Clifford, J. Cioslowski, B.B. Stefanov, G. Liu, A. Liashenko, P. Piskorz, I. Komaromi, R.L. Martin, D.J. Fox, T. Keith, M.A. Al-Laham, C.Y. Peng, A. Nanayakkara, M. Challacombe, P.M.W. Gill, B. Johnson, W. Chen, M.W. Wong, C. Gonzalez, J.A. Pople, Gaussian 03, Revision C.02, Gaussian, Inc., Pittsburgh, PA, 2004.
[25] M.P. Badenes, C.J. Cobos, J. Mol. Struct. (THEOCHEM) 814 (2007) 51.
[26] M.J. Frisch, J.A. Pople, J.S. Binkley, J. Chem. Phys. 80 (1984) 3265 (and references therein).
[27] A.D. Becke, J. Chem. Phys. 98 (1993) 5648.
[28] A.D. Becke, Phys. Rev. A 38 (1988) 3098.
[29] C. Lee, W. Yang, R.G. Parr, Phys. Rev. B 37 (1988) 785.
[30] A.G. Baboul, L.A. Curtiss, P.C. Redfern, K. Raghavachari, J. Chem. Phys. 110 (1999) 7650.
[31] J.E. Sicre, C.J. Cobos, J. Mol. Struct. (THEOCHEM) 620 (2003) 215.
[32] M.P. Badenes, A.E. Croce, C.J. Cobos, Phys. Chem. Chem. Phys. 6 (2004) 747.
[33] M.E. Tucceri, E. Castellano, A.E. Croce, C.J. Cobos, J. Argent. Chem. Soc. 93 (2005) 29.
[34] M.P. Badenes, A.E. Croce, C.J. Cobos, J. Phys. Chem. A 110 (2006) 3186.
[35] G.N. Merrill, M.S. Gordon, J. Chem. Phys. 110 (1999) 6154.
[36] D. Jung, J.W. Bozzelli, J. Phys. Chem. A 105 (2001) 5420.
[37] N. Sebbar, H. Bockhorn, J.W. Bozzelli, Phys. Chem. Chem. Phys. 5 (2003) 300.
[38] A.P. Scott, L. Radom, J. Phys. Chem. 100 (1996) 16502.
[39] A. Hermann, J. Niemeyer, H.-G. Mack, R. Kopitzky, M. Beuleke, H. Willner, D. Christen, M. Schäfer, A. Bauder, H. Oberhammer, Inorg. Chem. 40 (2001) 1672.
[40] D. Scheffler, I. Schaper, H. Willner, H.-G. Mack, H. Oberhammer, Inorg. Chem. 36 (1997) 339.
[41] R. Kopitzky, M. Beuleke, G. Balzer, H. Willner, Inorg. Chem. 36 (1997) 1994.
[42] J. Troe, J. Chem. Phys. 66 (1977) 4758.
[43] C.J. Cobos, J. Mol. Struct. (THEOCHEM) 714 (2005) 147.
[44] M.W. Chase Jr., NIST-JANAF Thermochemical Tables, fourth ed. J. Phys. Chem. Ref. Data 1998, Monograph No. 9.
[45] L.A. Curtiss, P.C. Redfern, D.J. Frurip, in: K.B. Lipkowitz, D.B. Boyd (Eds.), Reviews in Computational Chemistry, vol. 15, Wiley-VCH, New York, 2000, p. 147.
[46] W.J. Hehre, L. Radom, P.v.R. Schleyer, J.A. Pople, Ab Initio Molecular Orbital Theory, Wiley, New York, 1986.
[47] S.P. Sander, R.R. Friedl, D.M. Golden, M.J. Kurylo, G.K. Moortgat, P.H. Wine, A.R. Ravishankara, C.E. Kolb, M.J. Molina, B.J. Finlayson-Pitts, R.E. Huie, V.L. Orkin, Chemical Kinetics and Photochemical Data for Use in Atmospheric Studies; NASA/JPL Data Evaluation, JPL Publication 06-2 Evaluation No. 15; NASA, Pasadena, CA, November 20, 2006. Available from: <http://jpldata-eval.jpl.nasa.gov/>.
[48] J.M. Roberts, S.B. Bertman, Int. J. Chem. Kinet. 24 (1992) 297.
[49] H. Tanimoto, H. Akimoto, Geophys. Res. Lett. 28 (2001) 2831.

[50] IUPAC Subcommittee on Gas Kinetic Data Evaluation, Summary of Evaluated Kinetic and Photochemical Data for Atmospheric Chemistry, Section II – Organic Reactions, Web Version February 2006, by R.G. Hynes, S.M. Saunders, P. Cassanelli, G.D. Carver, R.A. Cox. Available from: <http://www.iupac-kinetic.ch.cam.ac.uk/>.
[51] S.W. Benson, Thermochemical Kinetics, second ed., Wiley, New York, 1976.
[52] N. Cohen, J. Phys. Chem. Ref. Data 25 (1996) 1411.
[53] IUPAC Subcommittee on Gas Kinetic Data Evaluation, Supplementary Information, Thermodynamic Data Guide, 2003, Web Version. Available from: <http://www.iupac-kinetic.ch.cam.ac.uk/>.